

Tunable fractional-order Fourier transformer

A.A. Malyutin

Abstract. A fractional two-dimensional Fourier transformer whose orders are tuned by means of optical quadrupoles is described. It is shown that in the optical scheme considered, the Fourier-transform order $a \in [0, 1]$ in one of the mutually orthogonal planes corresponds to the transform order $(2 - a)$ in another plane, i.e., to inversion and inverse Fourier transform of the order a .

Keywords: fractional Fourier transform, Fourier-transform order tuning, optical quadrupole.

1. Introduction

The Fourier transform (FT) is one of the main mathematical operations used in many fields in physics, technology, and radioelectronics. The application of the FT in optics allows one to consider the problems of diffraction, principles of image formation and processing, and pattern recognition from a unified point of view. The introduction of a concept of the fractional Fourier transform (FrFT) of the order $a = 2\psi/\pi$, which is represented in the integral form as

$$\mathcal{F}^a[f(x)] = \frac{\exp(i\psi/2)}{(i \sin \psi)^{1/2}} \times \int_{-\infty}^{+\infty} f(\xi) \exp\left[i\pi \frac{(x^2 + \xi^2) \cos \psi - 2\xi x}{\sin \psi}\right] d\xi,$$

and its realisation by optical methods [1, 2] have shown that virtually any optical scheme consisting of an arbitrary set of lenses represents one or another sequence of FrFTs [3, 4], while the classical FT scheme is only a particular case of the FrFT with the fractional order $a = 1$.

The FrFT was used in the last decade in the theory of laser resonators [5, 6] to analyse the propagation of light beams [5, 7, 8], in holography [9], and for processing optical [10, 11] and acoustic [12] signals. To analyse laser signals, it is promising to transfer the FrFT method from the spatially-angular domain to the time-frequency domain [13].

A.A. Malyutin A.M. Prokhorov General Physics Institute, Russian Academy of Sciences, ul. Vavilova 38, 119991 Moscow, Russia; e-mail: amal@kapella.gpi.ru

Received 1 February 2005; revision received 29 November 2005
 Kvantovaya Elektronika 36 (1) 79–83 (2006)
 Translated by M.N. Sapozhnikov

In a number of practical problems such as the signal recovery [14] and optical cryptography [15–17], it is essential to use tunable fractional Fourier transformers. By now several such schemes have been proposed [18–22]. One of them [22] uses a specific gradient microlens and apparently can have only limited applications. The authors of other schemes [20, 21] propose to change the FrFT order by varying the distance between the input and output planes of the device; these schemes cannot provide a continuous variation in the transform order [20]. It is useful to analyse in more detail schemes [18, 19] which use lenses with a variable focal distance because they employ, as the scheme proposed in this paper, an element with a variable optical power.

2. Tuning of a fractional-order Fourier transformer by means of lenses with a variable focus

Figure 1 shows the simplest scheme of a tunable fractional-order Fourier transformer (FOFT). Lens L1 with a variable focal distance f (the method of varying f is discussed in [18]) is placed between the input RP1 and output RP2 reference planes separated by the distance d . We assume that lens L1 is placed in the middle of the interval of length d , i.e., the scaled FrFT will not be considered [23]. The propagation of radiation from RP1 to RP2 is described by the $ABCD$ matrix, which can be expressed in terms of the optical parameters of the scheme or the main parameters of the FOFT:

$$T_{\text{FrFT}} = \begin{pmatrix} 1 - d/2f & d - d^2/4f \\ -1/f & 1 - d/2f \end{pmatrix} =$$

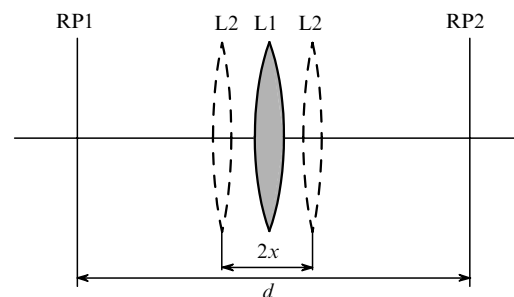


Figure 1. Optical scheme of the FOFT of type 1 with a single lens L1 or a two-component zoom lens L2; RP1 and RP2 are the base input and output planes, respectively.

$$= \begin{pmatrix} \cos \psi & f^* \sin \psi \\ -\sin \psi / f^* & \cos \psi \end{pmatrix}. \quad (1)$$

It follows from (1) that the accumulated Gouy phase (AGP) ψ [24] of the Gaussian eigenbeam* (whose wave fronts and dimensions coincide in RP1 and RP2) and its Rayleigh length f^* are

$$\psi = \arccos \left(1 - \frac{d}{2f} \right) = \frac{\pi a}{2}, \quad (2)$$

$$f^* = \frac{\pi w^2}{\lambda} = \left[d \left(f - \frac{d}{4} \right) \right]^{1/2}. \quad (3)$$

We obtain from (2) and (3) that matrices (1) describe the FOFT of type 1 (with the gap–lens–gap geometry) [2] only for $f > d/4$. The variation of f (at constant d) gives the tuning curve $\psi(d/f^*)$, which is presented in Fig. 2 (denoted by the letter E). The curve is plotted from the value $f = d/2$ by increasing the focal distance of the lens at each subsequent point by 25%. According to (2), to change the AGP from $\psi = 90^\circ$ ($f = d/2$, $a = 1$) up to $\psi = 10^\circ$ ($a \approx 0.11$), the focal distance of lens L1 should be increased by a factor of 66.

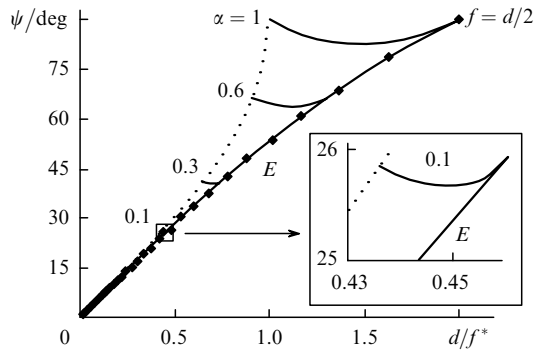


Figure 2. Tuning curves for the FOFT (Fig. 1) with a single lens with a variable focal length (curve E) and zoom lenses with different optical powers (values of the coefficient α are indicated). The dotted curve is the tuning curve for the optical scheme in Fig. 3.

The method of FOFT tuning with the help of a zoom lens described in [19] assumes the replacement of lens L1 by two components (Fig. 1) with the optical power $p = 4\alpha/d$, where $\alpha \leq 1$. For the distance between the components equal to $2x$ and their symmetric arrangement with respect to the middle of the segment d , the elements of matrix (1) take the form

$$\begin{aligned} A = D &= 1 - pd + \frac{p^2 x(d-2x)}{2}, \\ B &= d - \frac{p(d^2 - 4x^2)}{2} + \frac{p^2 x(d-2x)^2}{2}, \\ C &= -2p(1 - px). \end{aligned} \quad (4)$$

* The AGP value at the output of the optical system described by the $ABCD$ matrix for an arbitrary Gaussian beam with the radius w at the system input and the wave-front curvature ρ is determined by the relation $\tan \psi' = B\lambda / (A + B\rho)\pi w^2$.

If $\alpha = 1$, by varying the distance between components from zero to d , we obtain the symmetric (with respect to $2x = d/2$) tuning curve (Fig. 2) with the minimal value $\psi \approx 82.82^\circ$ for $d/f^* \approx 1.5$. As the optical power of components increases (the coefficient α decreases), the AGP tuning range decreases from $\Delta\psi \approx 7.2^\circ$ for $\alpha = 1$ down to $\Delta\psi \approx 0.16^\circ$ for $\alpha = 0.1$. Therefore, the use of a zoom lens provides a relatively narrow range of variation of the AGP and related FrFT order ($\Delta a = \Delta\psi/90^\circ$). Note that the AGP has the same value at the end points of the curves, and optical schemes correspond to the FOFT of type 1 for $2x = 0$ and type 2 for $2x = d$.

3. FOFT tuning by means of optical quadrupoles

Consider now the optical scheme of a FOFT placed between two tunable optical quadrupoles (a pair of cylindrical lenses with equal optical powers of the opposite signs located in series) OQ1 and OQ2 [25, 26] oriented identically** but with different mutual arrangement of cylindrical lenses in them (Fig. 3). The scheme operation is described by the product of the $ABCD$ matrices of three elements: OQ1, FOFT [matrix (1)], and OQ2. We have for both quadrupoles [26]:

$$T_{\text{OQ1,2}} = \begin{pmatrix} 1 & 0 \\ \mp P_{1,2} & 1 \end{pmatrix}, \quad (5)$$

where $P_{1,2} = \cos 2\varphi_{1,2}/F_0$ are the moduli of the optical power of OQs; $\mp F_0$ is the focal distance of cylindrical lenses; $\varphi_{1,2}$ are the rotation angles of lenses; the minus and plus signs in (5) and hereafter correspond to the xz and yz planes passing through the optical axis of the system. The matrix for a FOFT consisting of spherical lenses, as shown in Fig. 3***, has the form

$$\begin{aligned} T_{\text{FrFT}} &= \begin{pmatrix} 1-d/f & d \\ -(2-d/f)/f & 1-d/f \end{pmatrix} \\ &= \begin{pmatrix} \cos \psi & f^* \sin \psi \\ -\sin \psi / f^* & \cos \psi \end{pmatrix}, \end{aligned} \quad (6)$$

where $f^* = f[d/(2f-d)]^{1/2}$. For the entire optical system in Fig. 3, the product of matrices (5) and (6) gives

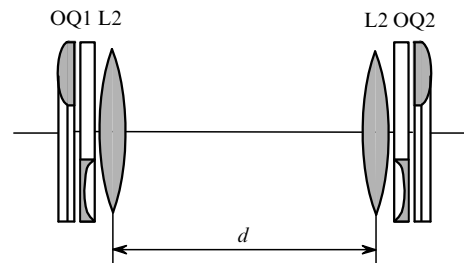


Figure 3. Scheme of the FOFT tunable with the help of optical quadrupoles OQ1 and OQ2.

** The optical power of both quadrupoles has the same sign in the same plane passing through the optical axis of the system (for example, xz).

*** According to the notation used in [2], we employ here the FOFT geometry of type 2 (lens–gap–lens), which provides a smaller optical path than the FOFT of type 1 (gap–lens–gap) (Fig. 1).

$$T_{xz,yz} = T_{\text{Oq2}} T_{\text{FrFT}} T_{\text{Oq1}}$$

$$= \begin{pmatrix} C \mp P_1 f^* S & S f^* \\ -S/f^* \mp C(P_1 + P_2) + P_1 P_2 f^* S & C \mp P_2 f^* S \end{pmatrix}, \quad (7)$$

where $C = \cos \psi$ and $S = \sin \psi$. Matrix (7) describes FrFT both in the xz and yz planes (scaled or without scaling) if

$$0 \leq (C \mp P_1 f^* S)(C \mp P_2 f^* S) \leq 1. \quad (8)$$

The analysis of (8) is considerably simplified by assuming that $\varphi_1 = \varphi_2$, i.e., that OQs at the input and output are completely identical: $P_1 = P_2 = P = \cos 2\varphi/F_0$. In this case, relation (8) can be written in the form

$$0 \leq C \mp \cos 2\varphi \frac{f^* S}{F_0} \leq 1. \quad (9)$$

The first corollary from (9) is trivial: taking (6) into account, it is necessary to fulfil the condition $|1 - d/f| < 1$ under which a system of spherical lenses separated by a gap and described by matrix (6) would be a FOFT; this gives the inequality $0 < d < 2f$. Another corollary concerns the restriction

$$F_0 \geq \frac{fd}{2f - d} \quad (10)$$

imposed on the relation between the parameters of optical elements of the scheme shown in Fig. 3. Here, we assume

that the entire range of the rotation angle of a cylindrical lens is used ($\varphi = 0 - 45^\circ$). Therefore, if condition (10) for this scheme is fulfilled, matrix (7) can be rewritten in the form

$$T_{xz,yz} = T_{\text{Oq2}} T_{\text{FrFT}} T_{\text{Oq1}} = \begin{pmatrix} \cos \Psi & F^* \sin \Psi \\ -\sin \Psi / F^* & \cos \Psi \end{pmatrix}_{xz,yz}. \quad (11)$$

Figure 4 presents the AGP $\Psi_{xz,yz}$ and the eigenbeam radius (normalised to $w_f = (\lambda f / \pi)^{1/2}$) of the tunable FOFT calculated for two sets of parameters f , d , and F_0 satisfying condition (10).

Note first of all that for both sets of parameters of the elements of the tunable FOFT there exists a singularity at the point $\varphi = 0$. For $\varphi = 0$, the eigenbeam size tends to infinity in the first case ($f = 100$ cm, $d = 120$ cm, and $F_0 = 150$ cm) in the xz plane and in the second case ($f = d = F_0 = 100$ cm) in both planes, and matrix (7) becomes equivalent to the $ABCD$ matrix of a segment of length d . Therefore, the scheme in Fig. 3 does not perform the two-dimensional FrFT for a beam of a finite size at the point $\varphi = 0$ for any set of parameters. In the second case, the only difference is that additional inversion takes place in the xz plane ($A = D = -1$).

For $d \neq f$, the fractional orders of the Fourier transforms performed in the xz and yz planes are not identical, so that for each fixed value of φ the scales of the field picture along the x and y axes at the FOFT output are different. This is demonstrated in Fig. 5, where the initial intensity distribution (Fig. 5a), which formally can be considered as the zero-order FT, and distributions corresponding to

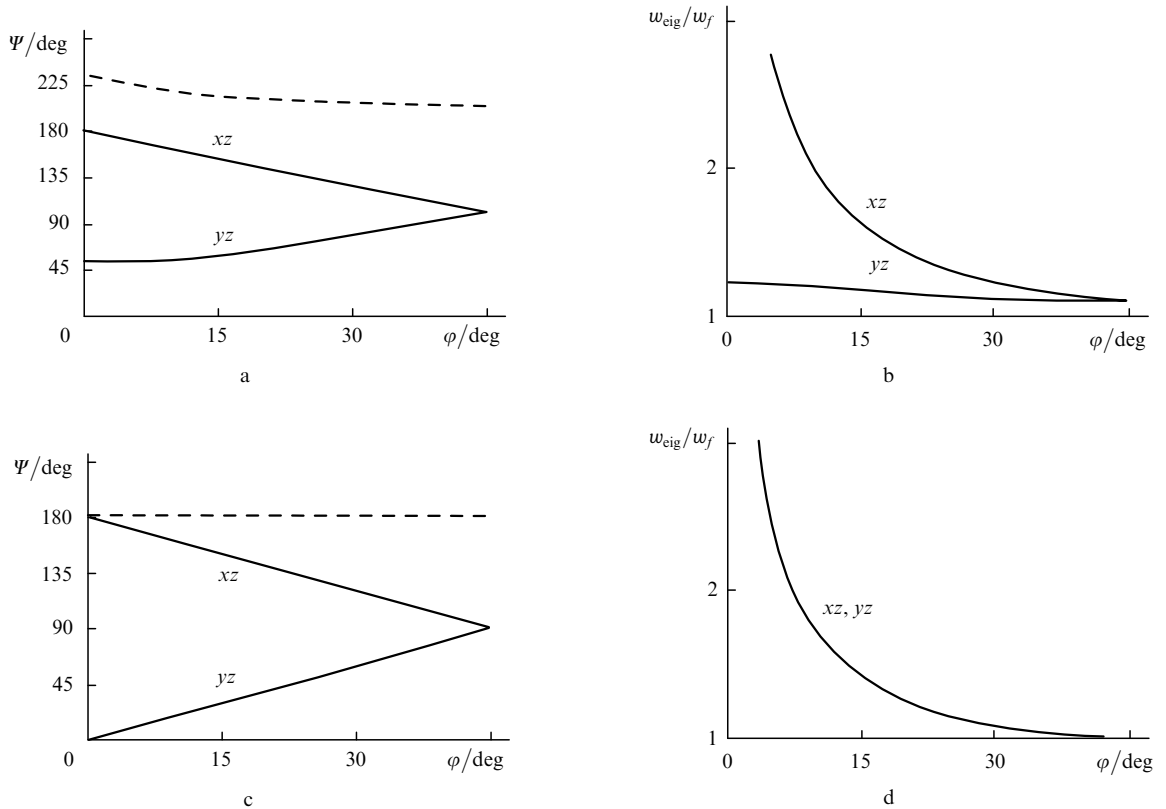


Figure 4. Dependences of the accumulated Gouy phase (a, c) and the normalised radius of the Gaussian eigenbeam (b, d) on the rotation angle of cylindrical lenses in OQ1 and OQ2 for the FOFT in Fig. 3 with parameters $f = 100$ cm, $d = 120$ cm, $F_0 = 150$ cm (a, b) and $f = d = F_0 = 100$ cm (c, d). The dashed lines show the dependences of the phase sum $\psi_{xz} + \psi_{yz}$ on the angle φ .

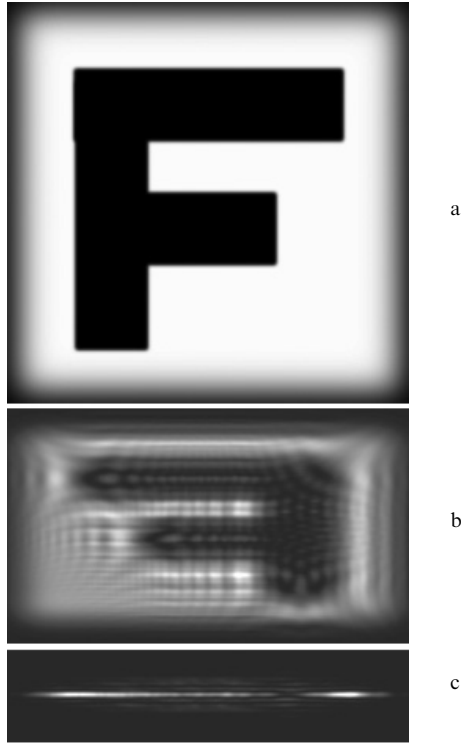


Figure 5. Radiation intensity distributions at the input (a) and output (b, c) of the tunable FOFT with parameters $f = 100$ cm, $d = 120$ cm, $F_0 = 150$ cm for $\varphi = 0$, $a_{xz} = a_{yz} = 0$ (the horizontal size of the figure is $L = 15$ mm) (a); for $\varphi = 20^\circ$, $a_{xz} = 1.6$, $a_{yz} = 0.73$, $L = 12.8$ mm (b); and for $\varphi = 37.76^\circ$, $a_{xz} = 1.26$, $a_{yz} = 1$, $L = 7.2$ mm (c).

$\varphi = 20^\circ$ and $\varphi \approx 37.8^\circ$ (Figs 5b, c) are presented. In the latter case, we have the FrFT of the order $a_{xz} = 1.26$ in the xz plane and the conventional FT (of the order $a_{yz} = 1$) in the yz plane.

By choosing $f = d = F_0 = 100$ cm, we obtain for all values of φ (except the singularity $\varphi = 0$) the scheme of a tunable two-dimensional FOFT with the $ABCD$ matrix

$$T_{xz,yz} = \begin{pmatrix} \mp \cos 2\varphi & f \\ -\sin^2 2\varphi/f & \mp \cos 2\varphi \end{pmatrix}. \quad (12)$$

In this case, the eigenbeam radii in both planes xz and yz prove to be the same (Fig. 4d):

$$w_{\text{eig}} = \left(\frac{\lambda f}{\pi \sin 2\varphi} \right)^{1/2}. \quad (13)$$

Because $\psi_{yz} = 2\varphi$, and $\psi_{xz} = \pi - 2\varphi$ (i.e., the operation performed in the xz plane can be considered as inversion plus the inverse FT), the FrFT orders are related as $a_{xz} + a_{yz} = 2$. The tuning curve $\psi(d/F^*)$ related to the yz plane is shown by the dotted curve in Fig. 2. It passes through points corresponding to the FOFT tuning by means of a zoom lens for the positions of components corresponding to $2x = d$.

Note that for $\varphi = 22.5^\circ$, the AGP difference in the xz and yz planes in the case $f = d = F_0$ is 90° , and for a Gaussian beam having a plane wave front, the radius $w = (2\lambda f/\pi)^{1/2}$, and axes rotated through 45° with respect to the x and y axes, the optical scheme in Fig. 3 is a converter of the Hermite–Gaussian laser modes to the Laguerre–Gaussian modes.

The operation of a tunable FOFT ($f = d = F_0 = 100$ cm) and a conventional lens converter (Fig. 1, the length f^* for each value of φ was chosen equal to the corresponding value of F^*) is compared in Fig. 6. One can see that transformations of the image of an object at the input performed in these two cases are identical, except the image

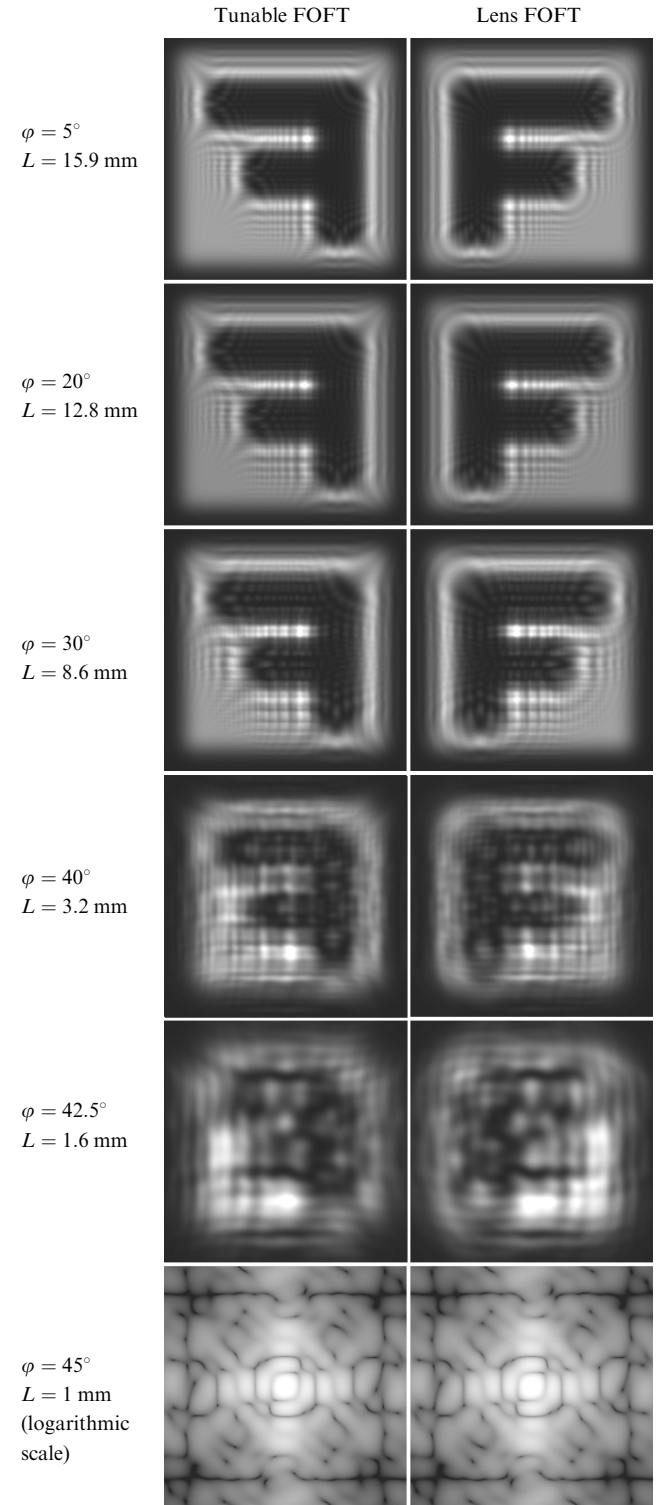


Figure 6. Radiation intensity distributions at the output of the tunable FOFT (Fig. 3) with parameters $f = d = F_0 = 100$ cm for different angles φ and different horizontal sizes L of the figures (left column) and of the corresponding lens FOFT (right column).

inversion performed in the tunable FOFT. As a result, the inversion and additional phase shift in the tunable FOFT give the diffraction structure of the beams which differs from that obtained with a usual converter, especially at the angles of the object imaging in coherent radiation, which was used in model calculations presented in Fig. 6. Indeed, for example, in the case of the Hermite–Gaussian mode u_{nm}^{HG} in the output reference plane, we have for the conventional FOFT of the order a :

$$\mathcal{F}_{xz}^a \mathcal{F}_{yz}^a [u_{nm}^{\text{HG}}] = \exp[-ia(n+m)\pi/2] u_{nm}^{\text{HG}}, \quad (14)$$

whereas for the tunable FOFT (Fig. 3), we have

$$\mathcal{F}_{xz}^{2-a} \mathcal{F}_{yz}^a [u_{nm}^{\text{HG}}] = \exp[-in\pi - ia(m-n)\pi/2] u_{nm}^{\text{HG}}, \quad (15)$$

i.e., the phase additions of the expansion terms of an arbitrary field in modes prove to be different.

4. Conclusions

In the general case, as shown in [18], the parameters of a light wave (scale, field curvature, and the FT order) can be controlled by using an optical scheme containing six cylindrical lenses with a variable focal distance. Such a device has not been realised so far. The FOFT schemes proposed earlier [18–22] have a limited tuning range of the FT order [18, 19] or require the change in the positions of the input and output planes of the device [20, 21]. The FOFT described in [22] belongs to fiberoptic devices. At the same time, the tunable two-dimensional fractional Fourier transformer proposed in this paper uses conventional optical elements (spherical and cylindrical lenses) and is quite simple. The transformer allows one to fix the positions of a source (the light-field distribution under study) and a detector, and the FrFT order [$a \in [0, 1]$ in one plane and $(2-a)$ in another plane] can be changed only by rotating the cylindrical components of optical quadrupoles around the optical axis of the device.

Acknowledgements. This work was supported by the Russian Foundation for Basic Research (Grant No 05-02-16818).

References

- Mendlovic D., Ozaktas H.M. *J. Opt. Soc. Am. A*, **10**, 1875 (1993); *ibid.*, 2522 (1993).
- Lohmann A.W. *J. Opt. Soc. Am. A*, **10**, 2181 (1993).
- Bernardo L.M., Soares O.D.D. *J. Opt. Soc. Am. A*, **11**, 2622 (1994).
- Ozaktas H.M., Erden M.F. *Opt. Commun.*, **143**, 75 (1997).
- Ozaktas H.M., Mendlovic D. *Opt. Lett.*, **19**, 1678 (1994).
- Zhao D. *Opt. Commun.*, **168**, 85 (1999).
- Brunel M., Coemmellec S. *Opt. Commun.*, **230**, 1 (2004).
- Hwang H.-E., Han P. *Opt. Commun.*, **245**, 11 (2005).
- Jin S., Bae Y.-S., Lee S.-Y. *Opt. Commun.*, **198**, 57 (2001).
- Dragoman D., Dragoman M. *Opt. Commun.*, **141**, 5 (1997).
- Yetik I.S., Kutay M.A., Ozaktas H.M. *Opt. Commun.*, **197**, 275 (2001).
- Zalevsky Z., Mendlovic D., Kutay M.A., Ozaktas H.M., Solomon J. *Opt. Commun.*, **190**, 95 (2001).
- Dragoman D., Dragoman M. *Opt. Commun.*, **145**, 33 (1998).
- Ertosun M.G., Atli H., Ozaktas H.M., Barshan B. *Opt. Commun.*, **244**, 61 (2005).
- Unnikrishnan G., Joseph J., Singh K. *Opt. Lett.*, **25**, 887 (2000).
- Zhang Y., Zheng C.-H., Tanno N. *Opt. Commun.*, **202**, 277 (2002).
- Hennelly B., Sheridan J.T. *Opt. Lett.*, **28**, 269 (2003).
- Erden M.F., Ozaktas H.M., Sahin A., Mendlovic D. *Opt. Commun.*, **136**, 52 (1997).
- Lohmann A.W. *Opt. Commun.*, **115**, 437 (1995).
- Dorsch R.G. *Appl. Opt.*, **34**, 6016 (1995).
- Andres P., Furlan W.D., Saavedra G., Lohmann A.W. *J. Opt. Soc. Am. A*, **14**, 853 (1997).
- Dragoman D., Brenner K.-H., Dragoman M., Bahr J., Krackhardt U. *Opt. Lett.*, **23**, 1499 (1998).
- Hua J., Liu L., Li G. *Appl. Opt.*, **36**, 8490 (1997).
- Erden M.F., Ozaktas H.M. *J. Opt. Soc. Am. A*, **14**, 2190 (1997).
- Nemes G., Siegman A.E. *J. Opt. Soc. Am. A*, **11**, 2257 (1994).
- Malyutin A.A. *Kvantovaya Elektron.*, **36**, 76 (2006) [*Quantum Electron.*, **36**, 76 (2006)].